Available online at www.sciencedirect.com
SCIENCE DIRECT
Thermochimica Acta 441 (2006) 156–161
thermochimica acta
www.elsevier.com/locate/tca

Pressure-scanning DTA measurements of the cubic–smectic C phase transition of 1,2-bis-(4-*n*-octyloxy)- and 1,2-bis-(4-*n*-dodecyloxy benzoyl)hydrazines

Yoji Maeda *, Hiroshi Yokoyama

Liquid Crystal Nanosystem Project, SORST, Japan Science and Technology Agency, TRC, 5-9-9 Tokodai, Tsukuba, Ibaraki 300-2635, Japan

Received 26 October 2005; received in revised form 7 December 2005; accepted 11 December 2005

Abstract

The pressure-scanning differential thermal analyzer (DTA) measurements of the cubic (Cub)–smectic C (SmC) transition of thermotropic cubic mesogens of 1,2-bis-(4-*n*-octyloxybenzoyl)- and 1,2-bis-(4-*n*-dodecyloxybenzoyl)hydrazine, BABH(8) and BABH(12), were performed at isothermal condition using a high-pressure differential thermal analyzer. BABH(8) showed the same endothermic peak of the Cub–SmC transition in the pressurizing process as on heating at isobaric condition. On the other hand, BABH(12) showed only the cubic phase between the crystal and the isotropic liquid under pressures up to 16–17 MPa, but a high-pressure smectic C (SmC(hp)) phase was induced instead of the cubic phase under higher pressure. The Cub–SmC(hp) phase transition with a small exothermic peak occurred in the pressurizing process and the transition was observed reversibly. The Cub–SmC(hp) phase transition was in accordance with the morphological and structural observations mentioned before. The strange phenomenon of the inversion of sign of the Cub–SmC transition heat of BABH(*n*) homologues can be explained by the "Alkyl-chains as entropy reservoir" mechanism proposed by Saito et al.

Keywords: Thermotropic cubic mesogen BABH(12); Pressure-scanning DTA mesurement; Cubic-high-pressure smectic C phase transition; Inversion of sign in the transition heat

1. Introduction

Since the discovery of thermotropic cubic mesophase of 4′-*n*-hexadecyloxy- and 4′-*n*-octadecyloxy-3′-nitrobiphenyl-4-carboxylic acid, referred to as ANBC(16) and ANBC(18), respectively, in 1957 [1], a number of thermotropic cubic mesogens have now been reported [2]. Some thermotropic cubic mesogens show the crystal (Cr)–smectic C (SmC)–cubic (Cub)–isotropic liquid (I) phase sequence under atmospheric pressure. Schubert et al. [3] synthesized 1,2-bis-(4-*n*-alkyloxybenzoyl)hydrazines in 1978, denoted as BABH(*n*), where *n* indicates the number of carbon atoms in the alkoxy chain. As reported by Demus et al. [4], the octyloxy-, nonyloxy- and decyloxy-homologues of the BABH(*n*) series exhibit both the cubic and smectic C phases, and show the Cr–Cub–SmC–I phase sequence. Interestingly, the order of phases (Cub–SmC) is reversed in comparison to that (SmC–Cub) found for ANBC(*n*) and other compounds [5–13]. The chemical structure of BABH(*n*) compound is,

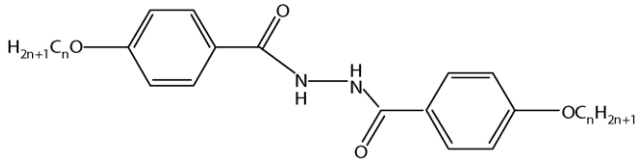

The molecules have two terminal alkoxy chains and a hydrazine core at molecular center, which form sheets linked by intermolecular hydrogen bond in the crystalline state and mesophases [9]. Recently BABH(11), BABH(12) and BABH(14) with longer alkyl chains ($n > 10$) were synthesized by Kutsumizu and coworkers [14] and these compounds showed only the cubic phase between the crystal and the isotropic liquid.

The authors have been studied the phase behaviour of a homologous series of the hydrazine compounds, BABH(8), BABH(10), BABH(11) and BABH(12) under pressure using a high-pressure differential thermal analyzer (DTA), a polarizing

* Corresponding author. Tel.: +81 29 847 9818; fax: +81 29 847 9819.
E-mail address: maeda@nanolc.jst.go.jp (Y. Maeda).

0040-6031/$ – see front matter © 2005 Published by Elsevier B.V.
doi:10.1016/j.tca.2005.12.015

optical microscope (POM) equipped with a high-pressure optical cell, and a wide-angle X-ray diffraction equipped with a pressure vessel and reported the T versus P phase diagrams [15–17]. Since the Cub–SmC transition lines of BABH(8) and BABH(10) have a negative slope (dT/dP) in the T versus P phase diagrams, the temperature range for the cubic phase decreased rapidly with pressure. The triple point for the SmC, Cub and Cr phases was estimated as 31.6 MPa, 147 °C in BABH(8) and 10–11 MPa, 144 ± 1 °C in BABH(10), which indicate the upper limit of pressure for the observation of the cubic phase. The cubic phase exists only in the low-pressure region and the Cr–Cub–SmC–I phase sequence changes to the Cr–SmC–I sequence in the high-pressure region. On the other hand, BABH(11) and BABH(12) show only the cubic phase between the crystal and isotropic liquid under atmospheric pressure [14]. However, applying hydrostatic pressure on the samples induced the formation of high-pressure smectic C (SmC(hp)) phase instead of the cubic phase at pressures above 10–11 MPa for BABH(11) and 16–17 MPa for BABH(12), respectively [17]. So the Cr–Cub–I phase sequence in the low-pressure region changed sharply to the Cr–SmC(hp)–I sequence in the high-pressure region. The formation of the SmC(hp) phase was confirmed using the POM texture observation and X-ray diffraction measurements under hydrostatic pressures [17]. The structure and optical texture between the cubic and the usual SmC or high-pressure SmC(hp) phases changed reversibly from the spot-like X-ray pattern and the dark field of view for the cubic phase to the Debye–Scherrer ring and the Schlieren texture for both the usual SmC and SmC(hp) phases. But unfortunately the Cub–SmC(hp) transition of BABH(11) and BABH(12) could not be detected using a usual high-pressure DTA method, because of almost vertical Cub–SmC(hp) transition lines in the T versus P phase diagrams.

In this paper, we report the experimental results of the transition between the cubic and the usual SmC or high-pressure SmC(hp) phases of BABH(8) and BABH(12), using a high-pressure DTA apparatus combined with a pressure-scanning DTA method.

2. Experimental

2.1. Sample preparation and characterization

BABH(8) and BABH(12) samples used in this study were prepared as described elsewhere [13,14]. The samples were characterized by using a Perkin-Elmer DSC-7 differential scanning calorimeter (DSC), a Leitz Orthoplan polarizing optical microscope (POM) and a Rigaku Rotaflex RU-200 wide-angle X-ray diffractometer (WAXD). DSC measurements were performed at a scanning rate of 5 °C min^{-1} under N_2 gas flow. Temperatures and heats of transition were calibrated using the standard materials, indium and tin. Transition temperatures were determined as the onset temperature of the transition peaks at which the tangential line of the inflection point of the rising part of the peak crosses over the extrapolated baseline. Morphological characterization was performed using a POM equipped with a Mettler hot stage FP-82.

2.2. DTA measurements under pressure

The high-pressure DTA apparatus used in this study is described elsewhere [18,19], but it is shortly explained as follows. The DTA system was operated in a temperature region between room temperature and 170 °C under hydrostatic pressure up to 100 MPa. Dimethylsilicone oil with a medium viscosity (100 cSt) was used as the pressurizing medium. Sample of about 4 mg was put inside the sample cell and coated with epoxy adhesives for the setting of the sample in the cell. The coating with epoxy adhesives prevented direct contact of the sample with the silicone oil. The Cub–SmC transition of BABH(8) is endothermic as it was shown by usual DSC measurements under atmospheric pressure [4]. The Cub–SmC transition under pressure was also detected using a high-pressure DTA technique and polarizing optical microscope equipped with a high-pressure optical cell at isobaric condition [15]. On the other hand, the usual DTA method failed to detect the Cub–SmC(hp) phase transition of BABH(12) in isobaric condition [17], although the POM texture observation and WAXD structural analysis showed clearly the existence of the Cub–SmC(hp) phase transition. So we applied the pressure-scanning DTA method to observe thermally the Cub–SmC(hp) transition in isothermal condition. Fig. 1 shows the block diagram of the high-pressure DTA apparatus used in this study [19]. The oil reservoir is used usually to adjust (either automatically or manually) a pressure change during the isobaric DTA measurements on heating or cooling processes. In the pressure-scanning DTA method, however, the oil reservoir with an electric furnace was used as a secondary pump of thermal pressure, and the pressure-scanning DTA measurements were performed in an isothermal condition of sample under any preset pressure. Thermal pressure was generated slowly by volume expansion or contraction of the silicone oil by heating or cooling the oil reservoir manually. At first the sample was heated to an appropriate temperature (148–155 °C) for the cubic phase at low pressures of 5–7 MPa as in the usual DTA measurements and holding the cubic phase isothermally for about 5–10 min to assure thermal equilibrium. Then the pressure-scanning DTA measurements started at a preset isothermal condition. Thermal pressure change was generated smoothly and linearly by volume expansion or contraction of silicone oil and thermal pressure ranged in a relatively narrow width of 30–40 MPa in this study. Since both pressurizing and depressurizing was set at a relatively small rate, i.e., 1–2 MPa min^{-1}, the manual control of change in pressure was successful.

3. Results and discussion

BABH(8) and BABH(10) show reversibly the Cr–Cub–SmC–I phase transition at low pressures below 32 MPa. Then the cubic phase disappears at higher pressures, while the SmC phase still exists in the high-pressure region [15,16]. On the other hand, BABH(11) and BABH(12) show only the cubic phase between the crystal and isotropic liquid in the low-pressure region up to 11–12 and 16–17 MPa, respectively [17]. Surprisingly a new mesophase closely resembled to the SmC phase of BABH(8),

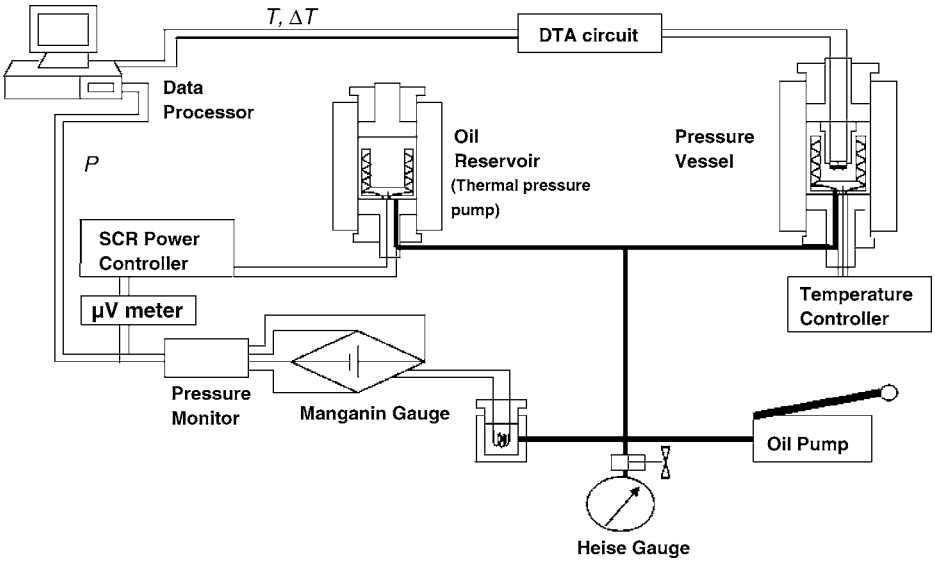

Fig. 1. Block diagram of a high-pressure DTA system [19]. The pressure-scanning DTA method uses the oil reservoir with an electric furnace as a thermal pressure pump.

denoted here as SmC(hp), is pressure-induced instead of the cubic phase under higher pressures [17]. Fig. 2 shows the T versus P phase diagrams of (I) BABH(8) and (II) BABH(12) obtained from the high-pressure DTA and POM texture observations. Arrows in the figures show the (a) isobaric and (b) isothermal pressure-scanning routes of DTA measurements used in this study.

Fig. 3 shows two DTA curves of BABH(8): (a) a heating curve at 5 °C min^{-1} and 10 MPa in the isobaric condition, and (b) a DTA curve at a rate of pressure increasing of ca. 1 MPa min^{-1} at 152 °C. It is noted here that both the DTA curves exhibit an endothermic peak of the cubic–SmC phase transition. This is reasonable from the T versus P phase diagram of BABH(8) because the thermodynamic relation between the cubic and the SmC phases is invariant at the isobaric and isothermal routes. Generally speaking, the DTA heating curves of BABH(12) show only two transitions of the crystal melting and isotropization at all pressures. The mesophase was an optically isotropic cubic phase in the low-pressure region below 16–17 MPa, while it was the SmC(hp) phase in the high-pressure region. Fig. 4 shows two DTA curves of BABH(12): (a) a heating curve at 5 °C min^{-1} and 23 MPa in the isobaric condition and (b) a DTA curve at a pressure-scanning rate of ca. 2 MPa min^{-1} at 150 °C. Both the DTA curves show large double peaks of the Cr_2–Cr_1 and Cr_1–Cub transition. In addition the (a) curve exhibits a small endothermic peak of the SmC(hp)–I transition at 23 MPa. In the (b) curve the melting transition was seen in the preheating process at 6 MPa. A pressure-scanning DTA measurement started after holding the cubic phase for 5 min at 150 °C. A small exothermic peak was observed at about 19 MPa on pressurizing and an endothermic peak at 17 MPa on the subsequent depressurizing processes. This transition was consistent with the Cub–SmC(hp) transition which was already shown by the morphological and structural observations of BABH(12) described before [17]. It is noted here that the thermal behaviour of BABH(12) exhibits the inverse sign of the Cub–SmC phase transition of BABH(8). The pressure-scanning DTA measurements of BABH(12) were performed in the temperature region between 148 and 155 °C. The exothermic peak of the Cub–SmC(hp) transition was commonly observed on pressurizing the cubic phase at isothermal condition and also the reversible transition was confirmed in the pressure-scanning mode. Fig. 5 shows the relation between observed pressure of the Cub–SmC(hp) transition of BABH(12) and temperature in isothermal condition. A horizontal or slightly positive slope of the Cub–SmC(hp) transition was obtained at 18–19 MPa. In any way, a sharp boundary exists between the cubic and SmC(hp) phases at about 18 ± 1 MPa, which is consistent with the POM observations: the texture changed from the cubic to SmC(hp) phases at 16–17 MPa.

Since the pressure-induced SmC(hp) phase of BABH(12) shows the same morphological and structural properties as those of the usual SmC phases of BABH(8) and BABH(10), we assume that the Cub–SmC(hp) transition of BABH(12) can be handled in the same manner as the usual Cub–SmC transition for BABH(8) and BABH(10). The exothermic Cub–SmC(hp) transition of BABH(12) looks apparently strange because the endothermic Cub–SmC transitions of BABH(8) and BABH(10) on heating are the clear experimental facts at atmospheric and low pressures. However, such strange phenomenon was estimated in terms of chain length dependence of the entropies of transition of BABH(n) homologues by Saito et al. [20–22]. Fig. 6a shows the measured values of entropy for the Cub–SmC transition of BABH(n) and for the SmC–Cub transition of ANBC(n) homologues as a function of number of the paraffinic carbon atoms. A negative value (□) of ΔS for the Cub–SmC transition of BABH(12) can be estimated by extrapolating the entropy line of BABH(8) and BABH(10). Of course this estimation can be proved only if the SmC phase of BABH(12) would be realized under atmospheric pressure. The verification was made fortunately by the observation of the exothermic Cub → SmC(hp) transition of BABH(12) in this study. Fig. 6a also suggests that BABH(n) homologues with more

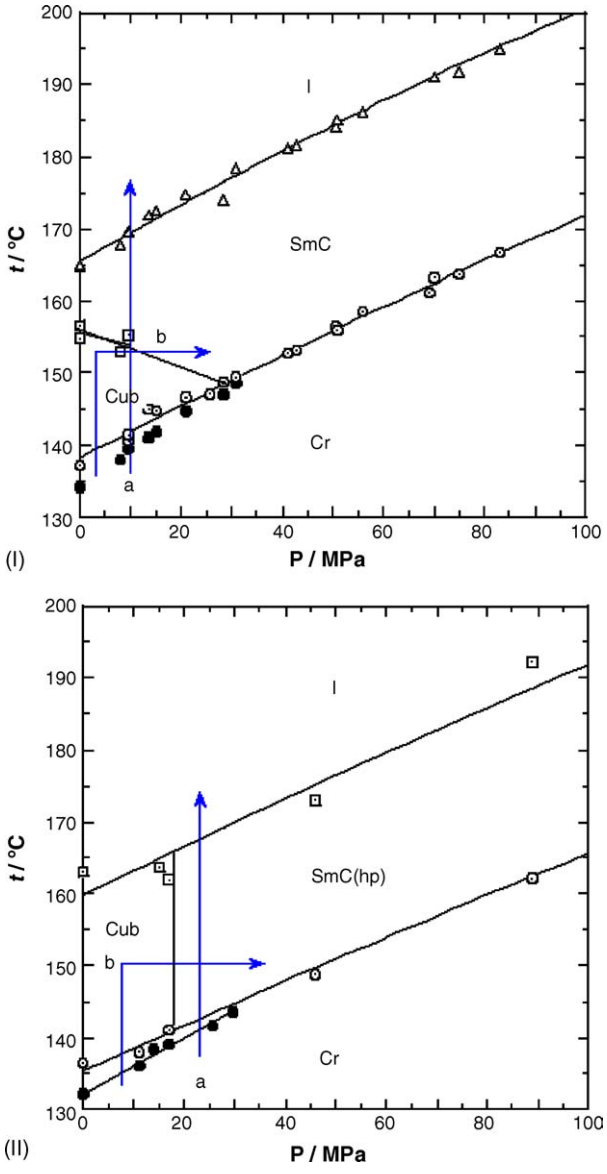

Fig. 2. T vs. P phase diagrams of: (I) BABH(8) [15] and (II) BABH(12) [17]. Letters 'a' and 'b' in the figures indicate the isobaric heating from the crystalline states and the isothermal pressurizing from the cubic to SmC phases, respectively.

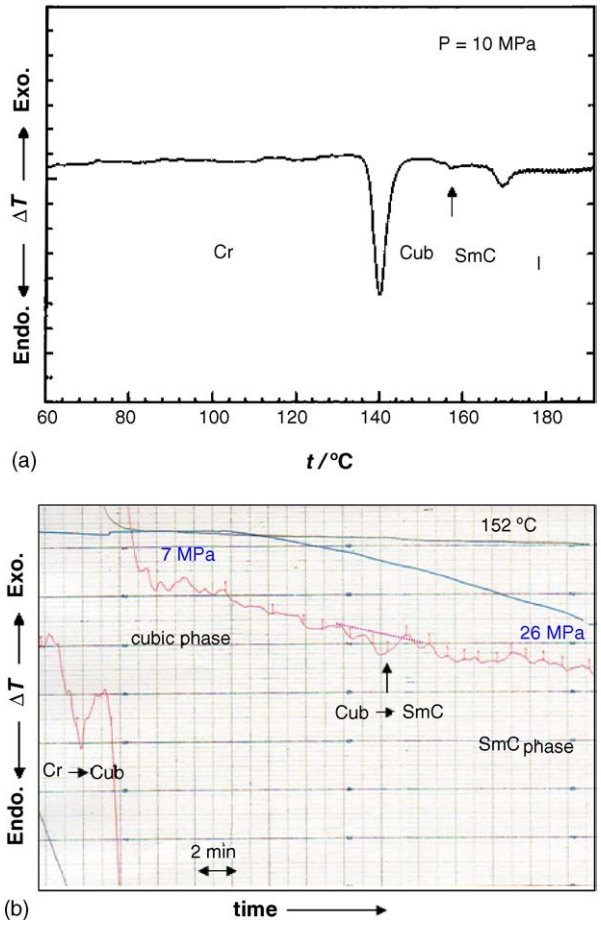

Fig. 3. Two DTA curves of BABH(8): (a) (*isobaric*) heating curve at 5 °C min^{-1} and 10 MPa and (b) (*isothermal*) pressure-scanning curve of the usual Cub–SmC transition at 152 °C and the pressure-scanning rate of about 1 MPa min^{-1} in the pressure region from 7 to 26 MPa.

longer alkyl chains have larger negative entropies of the Cub–SmC(hp) transition. For convenience, the relation of ΔS for the SmC → Cub transition, depicted as unified order of phase transition, is plotted in Fig. 6b as a function of total carbon number n_C of the paraffinic carbon atoms which are connected to the molecular core of BABH(n), ANBC(n) and bis(alkoxystilbazole)silver(I)dodecylsulphate complexes [23]. The positive slope of the ΔS–n_C relation of the three compounds suggest that the contribution of the alkyl chain to the transition entropy increases with increasing number of n_C. This means an increase of disorder of longer alkyl chains in the cubic phase [20–22]. The terminal alkoxy chains are highly disordered in the optically isotropic cubic phase whereas the spatial arrangement of the molecular core is more ordered. The opposite contributions of the terminal alkyl chains and the molecular core to the total entropy of transition can explain the inversion of the phase sequence between ANBC(n) (SmC → Cub on heating) and BABH(n) (Cub → SmC) [20–22]. Almost identical slope in Fig. 6b suggests that the terminal alkyl chains contribute similarly to the increase of the transition entropy with carbon number in ANBC(n), BABH(n) and bis(alkoxystilbazole)silver(I)dodecylsulphate complexes. Accordingly the terminal alkyl chains function as the reservoir for the entropy of the Cub–SmC transition which was proposed as the "Alkyl-chains as entropy reservoir" mechanism by Saito et al. [20–22]. Similar arguments about the contribution of peripheral alkyl chains to the transition entropy have been proposed for the behaviour of the columnar phase under pressure [24–26]. Peripheral longer alkyl chains of discotic mesogens play an important role in the formation of discotic columnar phases such as benzene-hexa-*n*-alkanoates [24,27,28], 2,3,6,7,10,11-hexa-*n*-alkoxytriphenylene [29–31] and bis[1,3-di(*p*-*n*-alkylphenyl)propane-1,3-dionato]copper(II) complex [32]. When such discotic liquid crystals were heated, the peripheral alkyl chains show excited molecular motions in the columnar phases, whereas the central aromatic part remains rigid. The alkyl chains already have a large amount of transi-

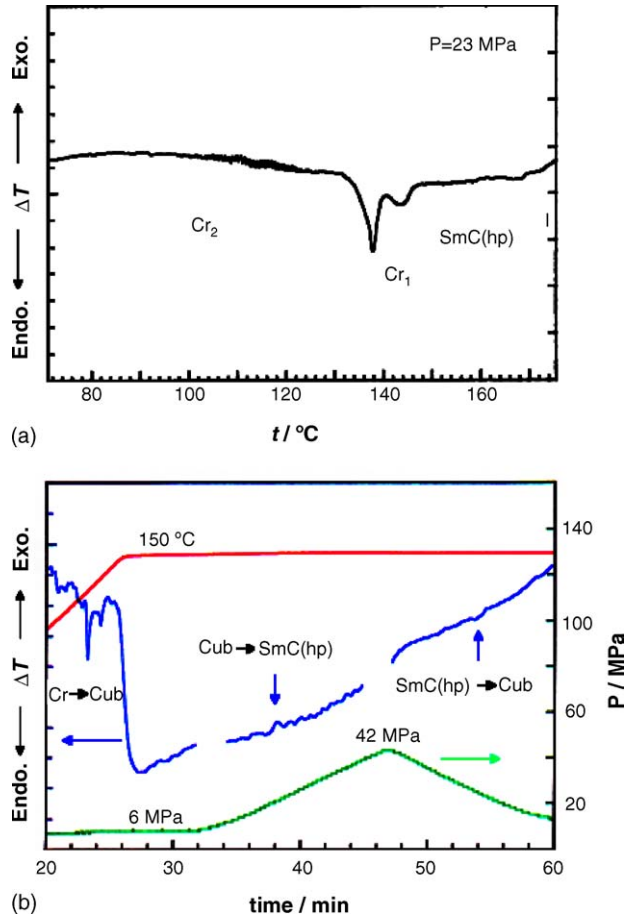

Fig. 4. Two DTA curves of BABH(12): (a) (*isobaric*) heating curve at 5 °C min^{-1} and 23 MPa and (b) (*isothermal*) pressure-scanning curve of Cub–SmC(hp) phase transition at 2 MPa min^{-1} in the pressure region from 6 to 42 MPa at 150 °C.

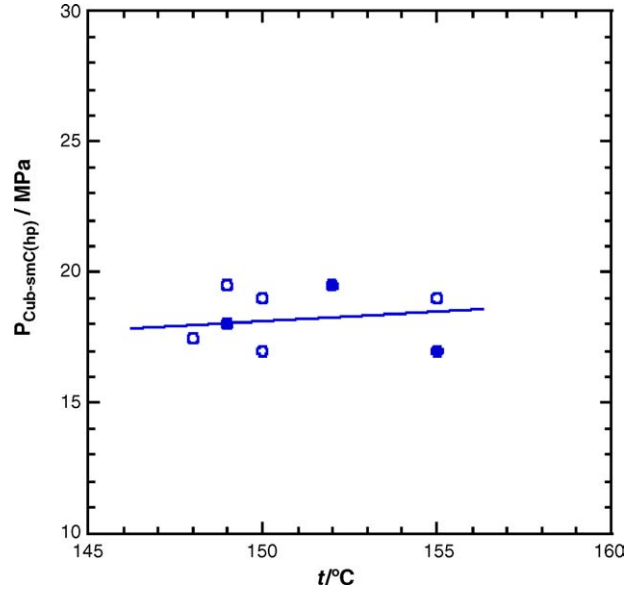

Fig. 5. The relation of the Cub–SmC(hp) transition pressure as a function of temperature in the isothermal condition. Open and filled circles indicate the transition in the pressurizing and depressurizing processes.

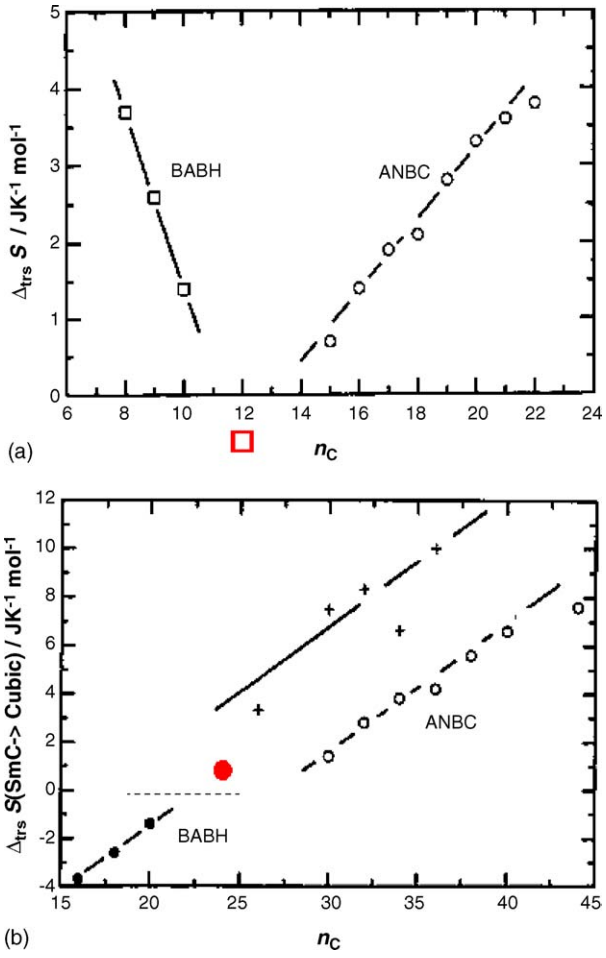

Fig. 6. (a) Observed entropy of transition between the SmC and the cubic phases of BABH(*n*) and ANBC(*n*) as a function of paraffinic carbon number n_C in the alkoxy chain. (b) Entropy of the SmC → Cub transition of (●) BABH, (○) ANBC and (×) bis(alkoxystilbazole)silver(I)dodecylsulphate complexes as a function of n_C that is the number of the paraffinic carbon atoms per molecular core [20,21]. Since ANBC molecules are dimerized via intermolecular hydrogen bonding between the carboxylic acid groups, n_C is twice the number of the paraffinic carbon atoms of ANBC molecule. The ΔS values for BABH(*n*) are negative, except for BABH(12), because of inversely plotting for the unified expression for the SmC → Cub transition. Symbols (□) and (●) are the expected ΔS values for BABH(12) by a linear extrapolation.

tion entropy due to conformational melting of the peripheral paraffinic moieties, which is consistent with the concept of "Alkyl-chains as entropy reservoir" mechanism [20–22]. So the concept of the "Alkyl-chains as entropy reservoir" mechanism may have a wide applicability of various kinds of liquid crystalline compounds.

In BABH(12) the positive contribution of entropy from the alkyl chains of disordering is predominant over the negative contribution of entropy from the central core of ordering. The entropic situation of BABH(12), in contrast to the BABH(*n*) homologues with shorter alkyl chains, is similar to those of ANBC(*n*) and bis(alkoxystilbazole)silver(I)dodecylsulphate complexes. In summary, the cubic-high-pressure smectic C phase transition of BABH(12) was confirmed thermally using a pressure-scanning DTA technique. The change from the endothermic to exothermic heat of the Cub–SmC transition was

found for the first time in the same BABH(*n*) homologues. The phenomenon of change of sign in the heat of Cub–SmC transition of BABH(*n*) homologues can be plausibly explained by the "Alkyl-chains as entropy reservoir" mechanism proposed by Saito et al. [20–22].

Acknowledgements

We would like to express sincere thanks to Prof. S. Kutsumizu of Gifu University for kindly supplying the BABH(12) sample. We also express sincere thanks to Prof. K. Saito of the University of Tusukuba for kindly supplying the BABH(8) sample and the valuable advice.

References

[1] G.W. Gray, B. Jones, F. Marson, J. Chem. Soc. (1957) 393.
[2] S. Diele, P. Göring, in: D. Demus, J.W. Goodby, G.W. Gray, H.-W. Spiess, V. Vill (Eds.), Handbook of Liquid Crystals, vol. 2B, Wiley-VCH, Weinheim, 1998, pp. 887–900.
[3] H. Schubert, J. Hauschild, D. Demus, S. Hoffmann, Z. Chem. 18 (1978) 256.
[4] D. Demus, A. Gloza, H. Hartung, A. Hauser, I. Rapthel, A. Wiegeleben, Cryst. Res. Technol. 16 (1981) 1445.
[5] D. Demus, G. Kunicke, J. Nielsen, H. Sackmann, Z. Naturforsch. 23 (1968) 84.
[6] D.W. Bruce, D.A. Dunmer, S.A. Hudson, E. Lalinde, P.M. Maitlis, M.P. McDonald, R. Orr, P. Styring, Mol. Cryst. Liq. Cryst. 206 (1991) 79.
[7] B. Donnio, B. Heinrich, T. Gulik-Krywicki, H. Delacroix, D. Guillon, D.W. Bruce, Chem. Mater. 9 (1997) 2951.
[8] S. Kutsumizu, R. Kato, M. Yamada, S. Yano, J. Phys. Chem. B 101 (1997) 10666.
[9] P. Göring, S. Diele, S. Fischer, A. Wiegeleben, G. Pelzl, H. Stegemeyer, W. Thyen, Liq. Cryst. 25 (1998) 467.
[10] K.E. Rowe, D.W. Bruce, J. Mater. Chem. 8 (1998) 331.
[11] B. Donnio, D.W. Bruce, J. Mater. Chem. 8 (1998) 1993.
[12] B. Donnio, D.W. Bruce, New J. Chem. (1999) 275.
[13] N. Morimoto, K. Saito, Y. Morita, K. Nakasuji, M. Sorai, Liq. Cryst. 26 (1999) 219.
[14] T. Ito, S. Kutsumizu, S. Naito, Preprint of Japan Liquid Crystal Society, Aomori, 2003, p. 247.
[15] Y. Maeda, K. Saito, M. Sorai, Liq. Cryst. 30 (2003) 1139.
[16] Y. Maeda, T. Ito, S. Kutsumizu, Liq. Cryst. 31 (2004) 623.
[17] Y. Maeda, T. Ito, S. Kutsumizu, Liq. Cryst. 31 (2004) 807.
[18] Y. Maeda, Thermochim. Acta 163 (1990) 211.
[19] Y. Maeda, M. Sorai (Eds.), Comprehensive Handbook of Calorimetry and Thermal Analysis, John Wiley & Sons Ltd., New York, 2004, pp. 386–388.
[20] K. Saito, A. Sato, N. Morimoto, Y. Yamamura, M. Sorai, Mol. Cryst. Liq. Cryst. 347 (2000) 249.
[21] K. Saito, T. Shinhara, M. Sorai, Liq. Cryst. 27 (2000) 1555.
[22] K. Saito, M. Sorai, Ekisho 5 (2001) 20.
[23] D.W. Bruce, D.A. Dunmur, S.A. Hudson, E. Lalinde, P.M. Maitlis, M.P. McDonald, R. Orr, P. Styring, A.S. Cherodian, R.M. Richardson, J.L. Feijoo, G. Ungar, Mol. Cryst. Liq. Cryst. 206 (1991) 79.
[24] S. Chandrasekhar, B.K. Sadashiva, K.A. Suresh, N.V. Madhusudana, S. Kumar, R. Shashidhar, G. Venkatesh, J. Phys. Colloq. C3 (1979) 120.
[25] D.S. Shankar Rao, V.K. Gupta, S. Krishna Prasad, M. Manickam, S. Kumar, Mol. Cryst. Liq. Cryst. 319 (1998) 193.
[26] K. Ohta, M. Ikejima, M. Moriya, H. Hasebe, I. Yamamoto, J. Mater. Chem. 8 (1998) 1971.
[27] S. Chandrasekhar, B.K. Sadashiva, K.A. Suresh, Pramana 9 (1977) 471.
[28] M. Sorai, H. Yoshioka, H. Suga, Mol. Cryst. Liq. Cryst. 84 (1982) 39.
[29] C. Destrade, M.C. Mondon, J. Malthete, J. Phys. Colloq. C3 (1979) 17.
[30] C. Destrade, N.H. Tinh, H. Gasparoux, J. Malthete, Mol. Cryst. Liq. Cryst. 71 (1981) 111.
[31] M. Sorai, S. Asahina, C. Destrade, N.H. Tinh, Liq. Cryst. 7 (1990) 163.
[32] K. Ohta, H. Muroki, A. Takagi, I. Yamamoto, K. Matsuzaki, Mol. Cryst. Liq. Cryst. 135 (1986) 247.